ORIGINAL ARTICLE Open Access

ISSN 2278-1404

International Journal of Fundamental & Applied Sciences

A field based 3D QSAR model of novel anti-microtubule agent noscapine and its derivatives

Seneha Santoshi and Pradeep Kumar Naik*

Department of Biotechnology and Bioinformatics, Jaypee University of Information Technology, Waknaghat, Solan-173234, Himachal Pradesh, India

Abstract

BACKGROUD & OBJECTIVE: Noscapinoids are a new class of microtubule binding compounds which show great promise as chemotherapeutic agents for the treatment of human cancers. To investigate the structural determinants of noscapinoids responsible for anti-cancer activity in order to design more potent derivatives, attempts were made to developed a 3D QSAR model based on "field point" descriptors using Forge V10 software(Cresset group).

METHODOLOGY: We have used 53 structurally diverse noscapinoids in a single panel and experimentally determined their IC_{50} value using human acute lymphoblastic leukemia cells (IC_{50} values vary from 1.2 to 56.0 µM). Molecular models of these compounds were built,energy minimizedand geometry optimized.The data set was randomly divided into 43 training and 10 test set molecules. Amino noscapine was considered as template molecule for the calculation of hydrophobic, steric, electrostatic and volume field points.These field based descriptors were used to align the training set molecules with the template molecule.A Partial Least Square (PLS) model was built based on field points using sphere exclusion algorithm.

RESULTS:A statistically significant model (R_{train}^2 = 0.884; R^2_{LOO} = 0.875) was obtained with the field point descriptors. The robustness of the QSAR model was characterized by the values of the internal leave-one-out cross-validated regression coefficient (R^2_{LOO}) for the training set and r_{test}^2 for the test set. The overall root mean square error (RMSE) between the experimental and predicted IC_{50} value was 1.75 and R_{test}^2 = 0.713, revealing good predictability of the QSAR model. The 3D QSAR model developed in this study shall aid further design of novel potent noscapine derivatives.

KEYWORDS: *Noscapnoids, anti-cancer activity, 3D QSAR, molecular fields.*

1. Introduction

Phthalideisoquinoline[(S)-3-((R)-4-methoxy-6-methyl-5,6,7,8-tetrahydro [1,3]dioxolo [4,5-g]isoquinolin-5-yl) -6,7-dimethoxyiso-benzofuran-1(3H)-one], also commonly known asnoscapine(Fig. 1) is an opium alka-loid, isolated from *Papaversomniferum*. It is a non-addictive derivative of opium. This agent is orally available and primarily used for its antitussive (cough-suppressing) effects[1, 2, 3].Recently noscapine (Figure I) and its derivatives are shown to binds with microtubules (MT) stoichiometrically and possesses anti-cancer activity [4,5].However, unlike other clinically used MT-binding drugs such as vincas (MT depolymerizing) and taxanes (MT over-polymerizing and bundling), noscapine simply suppresses the dynamics of MT assembly without changing the dimer/ polymer ratio. As a result of very slow MT dynamics, noscapine blocks cell cycle progression at mitosis (prometaphase), leading eventually to apoptotic cell death in many cancer cell types[4,5,6,7,8]. In addition, noscapine seems to be a poor substrate for the drug pumps because it remains effective against multidrug-resistant cancer cells[9].Although noscapine is cytotoxic in a variety of different cancer cell lines in the public library of the U.S. National Cancer Institute (60-cell screen), the IC_{50} values remain in the high micromolar ranges (21.1 to 100 µM). Opportunities must now be explored to acquire better and more effective deriva-tives. Indeed, some initial efforts have been quite encou[r]aging in which some more effective derivative of the lead com-pound noscapine have been designed , synthesized and tested [10,11,12,13].

With recent advances in combinatorial synthesis technology several thousand compounds can be rapidly synthesized, thus expanding the relevant chemical space. Hence, there is a need for predictive models like QSAR (Quantitative Structure Activity Relationship) that will prioritize compounds for screening, aid rational synthesis and facilitate lead identification. A QSAR model is useful in relating biological activity to physico-chemical and structural descriptors of compounds.Specifically 3D-QSAR model seems

Corresponding author
Full Address :
Department of Biotechnology and Bioinformatics, Jaypee University of Information Technology, Waknaghat, Solan-173234, Himachal Pradesh, India
Phone no. 91-1792-239384 , Fax. 91-1792-245362
E-mail: *pknaik1973@gmail.com*

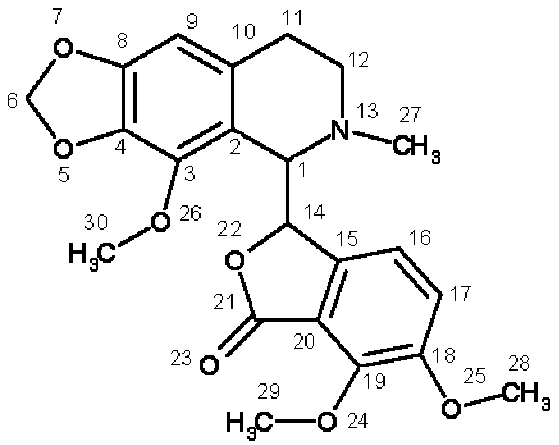

Figure I: Chemical structure of noscapine, which consists of an isoquinoline ring (top section) and a dimethoxyisobenzo-furanone ring (lower section)

to be more appropriate with better predictive accuracy for the newly designed compounds. A 3D-QSAR model is built by aligning three dimensional conformers of active compounds and subsequently used to score a candidate compound on the basis of a fitting function that evaluates the alignment of three dimensional chemical features to the model[14].

To investigate the structural determinants of noscapinoids responsible for anti-cancer activity, attempts were made to develop a 3D QSAR model utilizing "field point" descriptors using Forge V10 software (Cresset group).ForgeV10(Cresset group) is a new integrated approach to producing 3D QSAR models, utilizing "field point" descriptors[15].It uses molecular field sampling technique which has advantages over grid-based sampling methods used by many 3D QSAR model building programs. No parameterization of grid size or spacing needed. Moreover, the method is gauge invariant and reproducible and edge effectsare reduced as the sample positions are placed at the most important regions of space.We believe that our ligand-based approachesin identifying "field point" descriptors to develop 3D QSAR model will provide important insights that will lead to the design of novel noscapinoidsas anti-cancer agents.

2. Material and Methods

2.1 Biological data

We used 53 noscapine derivatives (TABLE 1) (commonly called as noscapinoids) that were synthesized in our laboratory[10,11,12,13] for QSAR model building. Anti-cancer activities of these compounds were measured against CEM, a multi-drug resistant human T-cell lymphoblastoid cell line under identical experimental conditions (to minimize bias)[16]. Cells were grown in RPMI 1640 medium (Mediatech, http:// cellgro.com) supplemented with 10% fetal calf serum, 1% antibiotics (penicillin/streptomycin), 2 mM 1-glutamine, at 37° C in a humidified atmosphere with 5% CO_2. Cell proliferation assay was performed in 96- well plates as previously described[12]. Briefly, cells were seeded in 100 µL growth medium at a density of 5 x 10^3 cells per well in 96-well plates and allowed to establish for 24 h. Serially diluted concentrations (0.01–500 µM) of noscapinoids were then added and cells were incubated for 72 h. We measured the inhibition of cell proliferation in a colorimeter by 3-(4,5-dimethylthiazol-2-yl)-5-(3-carboxymethoxyphenyl)- 2-(4-sulfophenyl)-2 H-tetrazolium inner salt (MTS) assay using the CellTiter96 AQueous One Solution Reagent (Promega, Madison, WI). Cells were incubated with MTS for 3 h and absorbance was measured at a wavelength of 490 nm using a microplate reader. The percentage of cell survival as a function of drug concentration was then plotted to determine the IC_{50} values (the drug concentration needed to prevent cell proliferation by 50%).

2.2 Molecular modeling

The builder feature in Maestro (Schrödinger package, version 8.5)[17]was used to build the molecular models of noscapine and its analogs. An appropriate bond was assigned to each structure order using ligprep (Schrödinger package, version 2.4)[18], and a unique low-energy ring conformation with correct chirality was generated. All structures were subjected to molecular mechanics energy minimizations using Macromodel (Schrödinger pack-age, version 9.8)[19] with default settings. OPLS 2005 force field was used to assign partial atomic charges to the molecular structures.We performed complete geometric optimiza-tion of these structures using Jaguar (Schrödinger package, ver-sion 7.7)[20] to ensure that the geometry of the structure was fairly reasonable. We have used hybrid density functional theory with Becke's three-parameter exchange potential and the Lee-Yang-Parr correlation functional (B3LYP)[21,22] and basis set 3-21G*[23,24,25]for geometrical optimization.

2.3 Compound alignment and 3D QSAR model building.

All the optimized structures along with their respected IC_{50} values were imported into Forge (version 10, Cresset)[26]for building field based 3D QSAR model.Out of 53 molecules , we selected 43molecules as a training set to build the model while the remaining 10 compounds served as a test set to evaluate the model.Amino noscapine was considered as template molecule for the calculation of field points. The field points were generated using XED (eXtended Electron Distribution) force field. Four differentmolecular fields such as positive and negative electrostatic, "shape" (van der Waals), and "hydrophobic" (a density function correlated with steric bulk and hydrophobicity) were calculated. A maximum of 200 conformations were generated for each molecule with long-distance electrostatics and attractive vdW forces turned off, forbetter conformation populations. Duplicate conformers were filtered using RMS threshold value of 0.5.All conformers found were minimized using the XED (eXtended Electron Distribution) force field with a gradient cut-off value of 0.1.

The training set molecules were aligned with the template molecule using maximum common substructure conformations generated for each molecule. A special conformation hunt was performed for all the training set molecules, where the common substructure with the reference molecule was held in the same conformation and groups that were not a part of the common substructure were again conformation hunted. The resulting conformations were then scored against the reference molecule using a scoring function which uses 50% field similarity and 50% Dice volume similarity. The top scoring conformations were presented as the top scoring alignments.

All the alignments were visually inspected to ensure the best possible model. The collective field points of the training set were used to derive a gauge invariant set of sampling points, which reduced the number of descriptors that needed to be considered, while ensuring that all regions around the molecule which might contribute to activity are adequately sampled.With a distance of 1Å between the sample points, sample values were calculated. A sphere exclusion algorithm was run to filter this set down, and then the field value for each molecule was calculated to generate a data matrix, on which partial least squares (PLS) regression was applied to generate a PLS model .

2.4 Model validation

The model was subjected to validation using test set data.The predictive capability of the developed QSAR model was validated based on several statistical tests. Prediction error sum of squares (PRESS) is a standard index to measure the accuracy of a modeling method based on the cross validation technique. The cross validation regression coefficient (R^2_{LOO}) was calculated based on the PRESS and SSY (Sum of squares of deviation of the experimental values from their mean) using following equation:

Table I: Chemical structures of noscapine and its congeners used in the present study, along with their observed inhibitory activity of cell proliferation (CEM cell line)

Sl No.	Compound Structure	IC_{50} (M)	Sl No.	Compound Structure	IC_{50} (M)
1	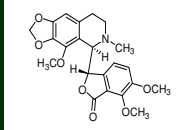	16.59 x 10^{-6}	2	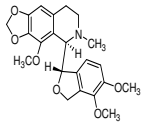	28.3 x 10^{-6}
3	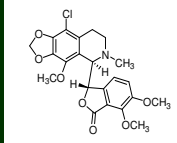	1.2 x 10^{-6}	4	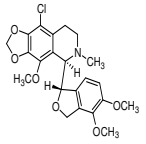	45.2 x 10^{-6}
5	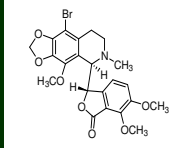	1.9 x 10^{-6}	6	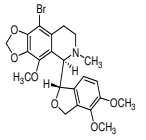	2.8 x 10^{-6}
7	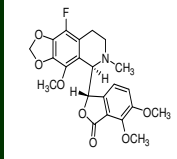	2.3 x 10^{-6}	8	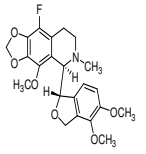	15.5 x 10^{-6}
9	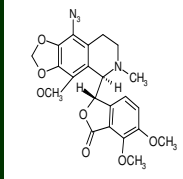	2.6 x 10^{-6}	10	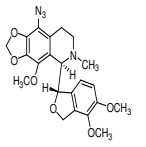	2.6 x 10^{-6}
11	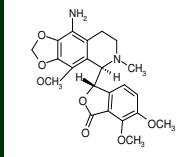	3.0 x 10^{-6}	12	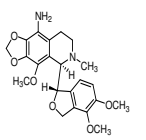	3.0 x 10^{-6}
13	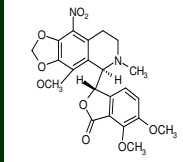	10.0 x 10^{-6}	14	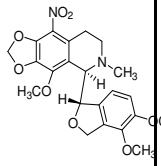	10.0 x 10^{-6}
15	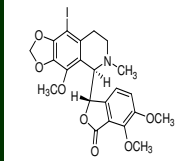	38.9 x 10^{-6}	16	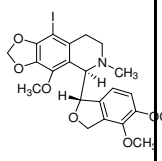	30.5 x 10^{-6}
17	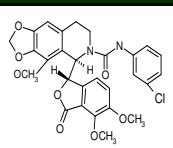	48.0 x 10^{-6}	18	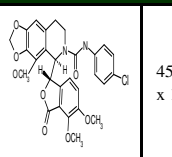	45.2 x 10^{-6}
19	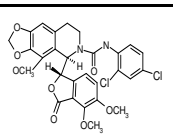	44.2 x 10^{-6}	20	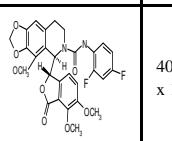	40.6 x 10^{-6}
21	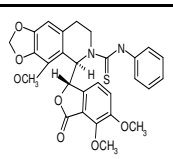	41.9 x 10^{-6}	22	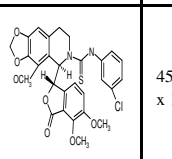	45.1 x 10^{-6}
23	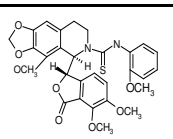	46.5 x 10^{-6}	24	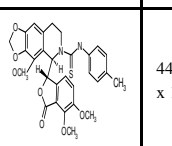	44.4 x 10^{-6}
25	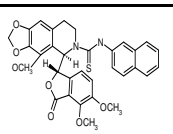	44.1 x 10^{-6}	26	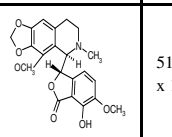	51.8 x 10^{-6}
27	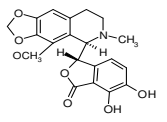	39.5 x 10^{-6}	28	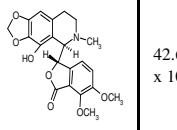	42.6 x 10^{-6}
29	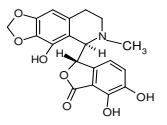	41.0 x 10^{-6}	30	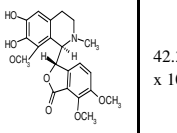	42.3 x 10^{-6}
31	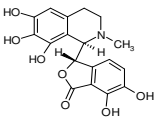	35.5 x 10^{-6}	32	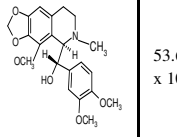	53.6 x 10^{-6}
33	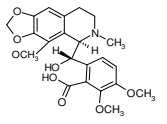	56.0 x 10^{-6}	34	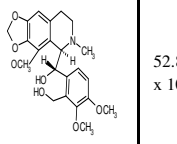	52.8 x 10^{-6}
35	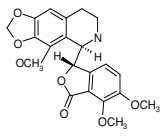	37.4 x 10^{-6}	36	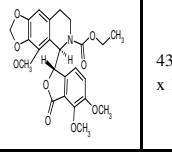	43.3 x 10^{-6}

$$R^2_{LOO} = 1 - \frac{PRESS}{SSY} = 1 - \frac{\sum_{i=1}^{n} (Y_{exp} - Y_{pred})^2}{\sum_{i=1}^{n} (Y_{exp} - \overline{Y})^2} \quad (1)$$

where, Y_{exp}, Y_{pred} and $\overline{Y}$ are the experimental, predicted and mean values of experimental activity, respectively of the training set compounds. Also, the accuracy of the prediction of the QSAR equation was validated by R^2

Int. J. Fundamental Applied Sci. Vol. 1, No. 4(2012) 81-87

and R^2_{adj}. The determination coefficient in prediction (R^2_{test}) was calculated using the following equation[27]:

$$R^2_{test} = 1 - \frac{\sum (Y_{pred_{test}} - Y_{test})^2}{\sum (Y_{test} - \overline{Y})} \quad (2)$$

where $Y_{pred_{test}}$ and Y_{test} are the predicted values based on the QSAR equation (model response) and experimental activity of the test set compounds. $\overline{Y}$ is the mean activity value of the training set compounds.

Sl No.	Compound Structure	IC_{50} (M)	Sl No.	Compound Structure	IC_{50} (M)
37	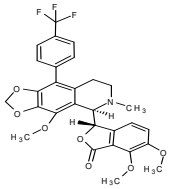	11.3 x 10^{-6}	46	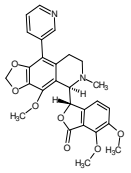	8.9 x 10^{-6}
38	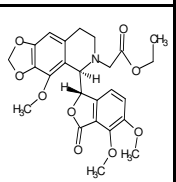	13.6 x 10^{-6}	47	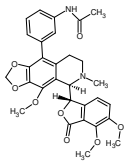	12.4 x 10^{-6}
39	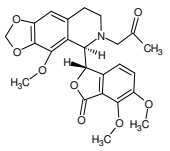	6.9 x 10^{-6}	48	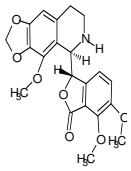	8.9 x 10^{-6}
40	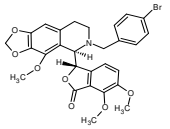	9.0 x 10^{-6}	49	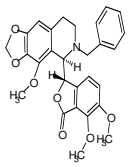	8.3 x 10^{-6}
41	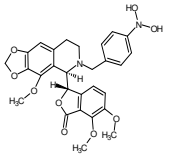	10.0x 10^{-6}	50	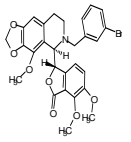	6.7 x 10^{-6}
42	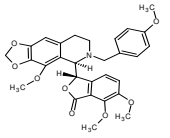	7.7 x 10^{-6}	51	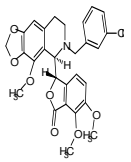	7.5 x 10^{-6}
43	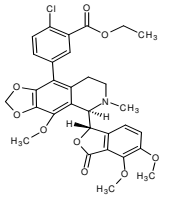	15.9 x 10^{-6}	52	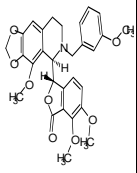	11.9 x 10^{-6}
44	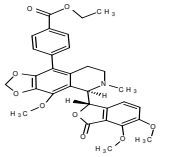	10.7 x 10^{-6}	53	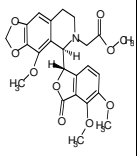	9.5 x 10^{-6}
45	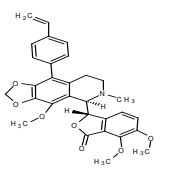	9.1 x 10^{-6}			

3. Results

The IC_{50} value of noscapinoids determined against human lymphoblastoid cells (CEM) was used as anti-cancer activity in evaluating the structure–activity relationships of noscapinoids quantitatively. Given a normal distribution (bellshapedcurve) of activity values of a set of compounds, the rule of thumb in developing fairly accurate QSAR models suggests that the difference between the highest and lowest biological activity of the compounds should be three to four orders of magnitude [28]. However, with the array of noscapinoids examined in this study, many of the compounds (22 out of 53) have weaker activity. Given this asymmetric distribution of activity, the actual range of raw experimental

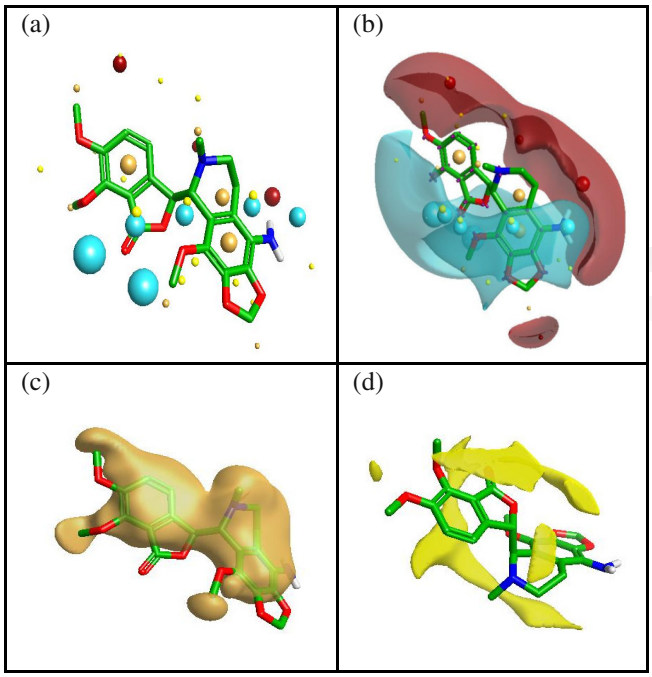

Figure II: Schematic representations of (a) different molecular field points of the template molecule(amino noscapine) Blue: Negative field points, Red: Positive field points, Yellow: Vander Walls surface field points,Gold/Orange: Hydrophobic field points. Large points indicate strong interactions and small fields showing less strong interactions. (b) Molecular Electrostatic Potential map of the reference molecule along with the field points.(c)hydrophobic surface map of the template molecule (d) Vander Walls surface map of the template molecule.

IC_{50}data in our case is, in fact is quite impressive (ranging from 1.2 to 56 µM, Table I) and can be reasonably used to assess the structure–activity relationship among noscapinoids. Noscapine derivatives 3, 5–7, 9–14and 37-53 have significantly better activities (IC_{50}< 16.0 µM) than the other compounds. On the contrary, derivatives 17–36 (aryl substituted N-carbamoyl/N-

thiocarbamoylnoscapine analogues) generally showed very weak or no activity.

We have divided the data set into training and test set compising of randomly selected 43 and 10 molecules respectively. Amino noscapine (molecule 11) is considered as template.The positive and negative electrostatic, "shape" (van der Waals), and "hydrophobic" (a density function correlated with steric bulk and hydrophobicity) fields were calculated for the template molecule (Figure IIa-d).

The training set molecules were aligned with the template molecule using maximum common substructure

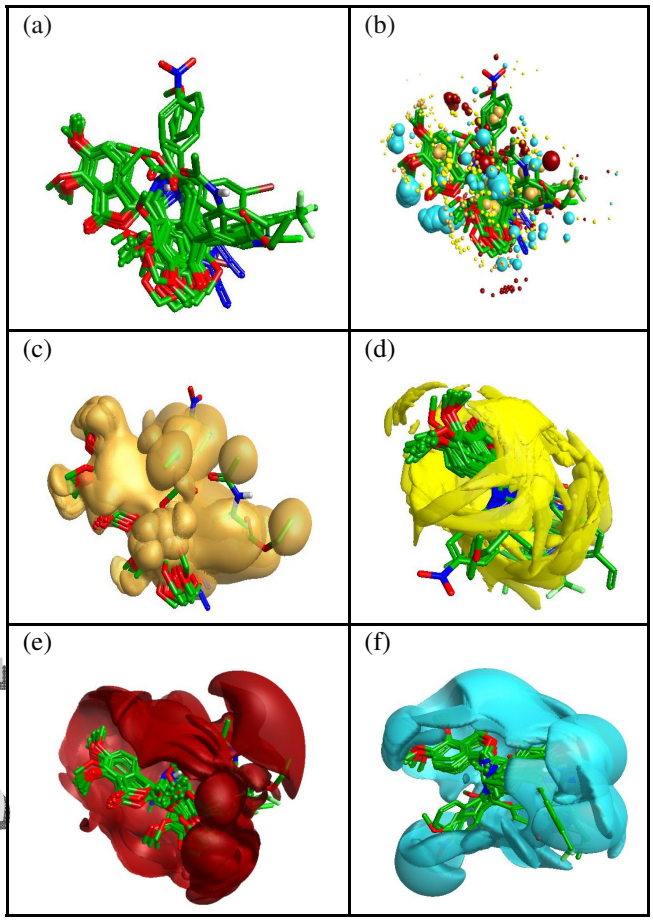

Figure III: Schematic representation of (a) the structure alignment of the top scoring conformatins of training set (b)after molecular field points are calculated for top scoring conformation of training set a reasonably good alignment of the training set field points with the template field points is visible. A sample of the field point positions is sampled out using a sphere exclusion algorithm. These are used to calculate the descriptors to be used for model generation.(c) showing the overall hydrophobic surface of the aligned set.(d)showing the overall Vander walls surface of the aligned set(e) the overall positive electrostatic surface of the aligned set(f) the overall negative electrostatic surface of the aligned set,all of them appear to be in synchronous with the template.

conformations generated for each molecule. After the conformation hunt the top scoring conformations are presented as the top scoring alignments.Molecular field points are calculated for the given set of molecules; the positive, negative, surface and hydrophobic molecular field points of the training set molecules were showeda reasonably good alignment with the reference field points (Figure IIIa-f). Further themolecular

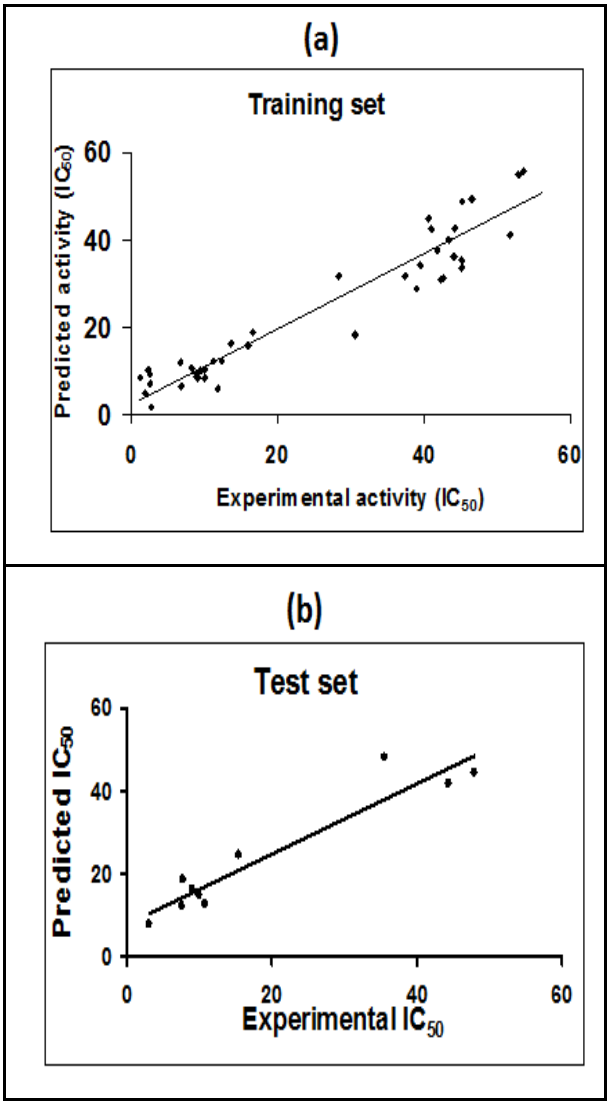

Figure IV: Relationship between experimental and predicted activities(IC_{50}) of (a) training set and (b) test set compounds based on 3D quantitative structure–activity relationship (QSAR) model; (R_{train}^2 = 88.4%),Q^2= 88.1% and determination coefficient (R^2_{test} = 71.3%) for the test set.

electrostatic Potential, hydrophobic and vander walls surface map generated for the aligned training set are in synchronous with the template.

A sample of the calculated field point positions of the alignment is sampled out using a sphere exclusion algorithm. These are used to calculate the descriptors to be used for model generation using PLS. The model was validated against the test set and determination coefficient (R^2_{test} for the test set was calculated to be 0.713 indicating high predictive ability of the model. The quality of the prediction models for the training set and test set com-pounds is shown in figure IVa-b.The alignment of the calculated molecular field points of the test set with the template molecule confirmed the reliability of the models shown in figure Va-f.

The QSAR model developed in this study is statistically best fitted (R_{train}^2= 0.884)for the prediction of antitumor activities (IC_{50}) of training and test sets of molecules, as reported in Table1. The quality of the prediction models for the training set and test set com-pounds as shown in Figure 4a-bis appreciable. The R^2 and R^2_{LOO} values (0.884 and 0.875) of the model corroborate the criteria for a highlypredictive QSAR model[29,30,31]and determination coefficient (R^2_{test} for the test set

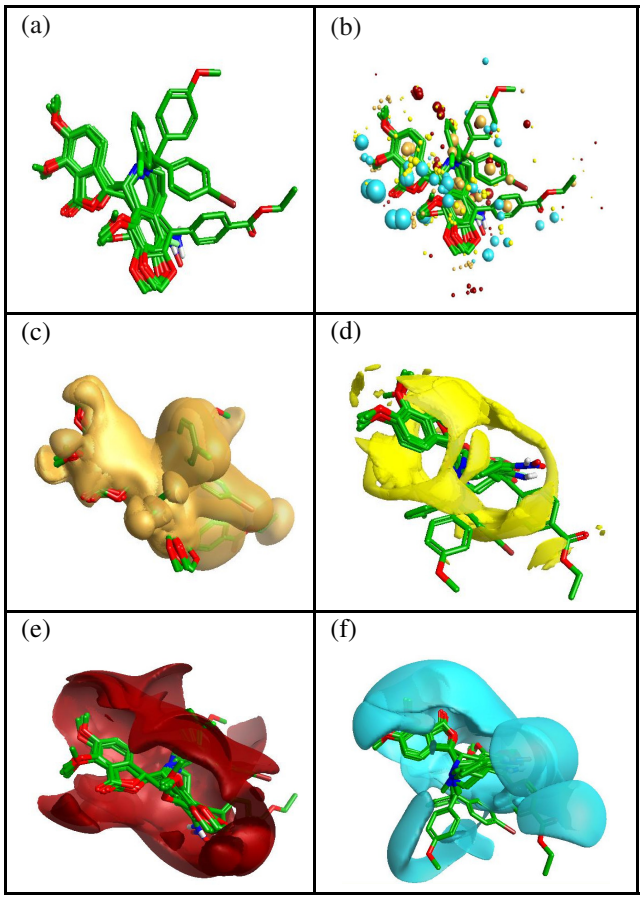

Figure V: Schematic representation of (a) the structure alignment test set molecules onto the template molecule (b)shows a reasonably good alignment of the test set field points with the reference field points.(c) showing the overall hydrophobic surface of thethealigned test set and template molecules(d)showing the overall Vander walls surface of the aligned test set and template molecules(e) the overall positive electrostatic surface of the aligned test set and template molecules (f) the overall negative electrostatic surface of the aligned test set and template molecules,all the surfaces and fields of the test set appear to be in sync with the template.

was calculated to be 0.713 indicating the reliability of the model. The standard error of estimate for the model was 0.159, which is an indicator of the robustness of the fit and suggests that the predicted IC_{50} based on QSAR model is reliable. Therefore, the QSAR model is highly predictive.

5. *Conclusion*

This body of work represents the first report of a highly predictive Field based 3D QSAR model of noscapine and its derivatives (noscapinoids). Modification of the properties in accordance with the results of this work by incorporating some structural features into the scaffold structure of noscapine will certainly achieve the final goal of improved anti-cancer noscapinoids.

Reference

1. Empey DW, Laitinen LA, Young GA, Bye CE & Hughes, DT, Comparison of the antitussive effects of codeine phosphate 20 mg, dextromethorphan 30 mg and noscapine 30 mg using citric acid-induced cough in normal subjects. *Eur j clin pharmacol*, **16** (1979)393-397
2. Chopra RN, & Mukherjee BI, Dikshit BB Narcotine: its pharmacological action and therapeutic uses. *Indian J Med Res,* **18** (1930) 35–49.
3. Karlsson M O, Dahlström B, Eckernäs SA, Johansson M & Alm AT, Pharmacokinetics of oral noscapine. *Eur j clin pharmacol* **39** (1990) 275-279.
4. Ye K, Ke Y, Keshava N, Shanks J, Kapp JA, Tekmal RR, Petros J, & Joshi HC, Opium alkaloid noscapine is an antitumor agent that arrests metaphase and induce apoptosis in dividing cells. *Proc Natl Acad Sci USA,* **95** (1998) 1601–1606.
5. Pradeep K N, Chatterji BP, Surya N V, Aneja R, Chandra R, Kanteveri S, & Joshi HC, .Rational design, synthesis and biological evaluations of amino-noscapine: A high affinity tubulin-binding noscapinoid. *J Comp Aided Drug Design*, **25** (2011) 443-454
6. Ye K, Zhou J, Landen JW, Bradbury EM, & Joshi HC Sustained activation of p34(cdc2) is required for noscapineinduced apoptosis. *J BiolChem* **276** (2001) 46697–46700.
7. Zhou J, Gupta K, Yao J, Ye K, Panda D, Giannakakou P, & Joshi HC, Paclitaxel resistant human ovarian cancer cells undergo c- Jun Nh2-terminal kinase-mediated apoptosis in response to noscapine. *J BiolChem* **277** (2002) 39777–39785.
8. Zhou J, Panda D, Landen JW, Wilson L, & Joshi HC Minor alteration of microtubule dynamics causes loss of tension across kinetochore pairs and activates the spindle checkpoint. *J Biol Chem,* **277** (2002) 17200–17208.
9. Aneja R, Liu M, Yates C, Gao J, Dong X, Zhou B, Vangapandu, S N, Zhou, J, & Joshi, H C, Multidrug Resistance-Associated Protein-Over Expressing Teniposide-Resistant Human Lymphomas undergo Apoptosis by a Tubulin-Binding Agent. *Cancer Res*, **68** (2008) 1495–1503.
10. Aneja R, Vangapandu SN, Lopus M, Viswesarappa V G, Dhiman N, Verma A, Chandra R, Panda D, & Joshi HC, Synthesis of Microtubule-Interfering Halogenated Noscapine Analogs Perturb Mitosis in Cancer Cells followed by Cell Death. *Biochem Pharmacol,* **72** (2006) 415–426.
11. Aneja R, Vangapandu SN, & Joshi HC, Synthesis and Biological Evaluation of a Cyclic Ether Fluorinated Noscapine Analog. *Bioorg Med Chem*, **14**(2006) 8352–8358.
12. Aneja R, Vangapandu SN, Lopus M, Chandra R, Panda D, & Joshi HC, Development of a Novel Nitro-Derivative of Noscapine for the Potential Treatment of Drug-Resistant Ovarian Cancer and T-Cell Lymphoma. *Mol. Pharmacol*, **69** (2006) 1801–1809.
13. Aggarwal S, Ghosh NN, Aneja R, Joshi HC, & Chandra R, A Convenient Synthesis of Aryl-Substituted N-Carbamoyl/N-ThiocarbamoylNarcotine and Related Compounds. *Helvetica Chimica Acta,* **85** (2002) 2458–2462.
14. Venkatarajan S M, Patel N, Bachmeier C, Mullan M, & Paris D, A 3D-QSAR model based screen for dihydropyridine-like compound library to identify inhibitors of amyloid beta (Aβ)production. *Bioinformation* , **5** (2010) 122-127.
15. Cheeseright T, Mackey M, Rose S, Vinter A, Molecular Field Extrema as Descriptors of Biological Activity: Definition and Validation. *J Chem Inf Model*, **46** (2006) 665-676.
16. Beck WT, & Cirtain MC, Continued expression of vinca alkaloid resistance by CCRF-CEM cells after treatment with tunicamycin or pronase. *Cancer Res* **42** (1982)184–189.

17. Schrödinger, LLC. Maestro, version 8.5, Schrödinger, LLC: New York, NY.
18. LigPrep, version 2.4, Schrödinger, LLC, New York, NY, 2010.
19. Macro Model, version 9.8, Schrödinger, LLC, New York, NY, 2010.
20. Schrödinger, LLC. Jaguar, version 7.7, Schrödinger, LLC: New York, NY.
21. Lee, C, Yang W, & Parr RG, Development of the Colle-Salvetti correlation-energy formula into a functional of the electron density. *Phys Rev B,* **37** (1988) 785-789.
22. Becke A D, A new mixing of Hartree-Fock and local density-functional theories. *J Chem Phys*, **98** (1993) 1372-1377.
23. Binkley J S, Pople JA, & Hehre W J, Self-consistent molecular orbital methods. 21. Small split-valence basis sets for first-row elements. *J Am Chem Soc,* **102** (1980) 939-947.
24. Gordon M S, Binkley J S, Pople J A, Pietro W J, & Hehre W J, Self-consistent molecular-orbital methods. 22. Small split-valence basis sets for second-row elements. *J Am Chem Soc*, **104** (1982) 2797-2803.
25. Pietro W J, Francl M M, Hehre W J, Defrees D J, Pople J A, & Binkley J S, Self-consistent molecular orbital methods. Supplemented small split-valence basis sets for second-row elements. *J Am Chem Soc*, **104** (1982) 5039-5048.
26. FORGE
27. Roy P P, & Roy K, On some aspects of variable selection for partial least squares regression models. *QSAR Comb Sci,* **27** (2008) 302–313.
28. Checchi PM, Nettles JH, Zhou J, Snyder JP, & Joshi HC Microtubule-interacting drugs for cancer treatment. *Trends PharmacolSci* **24** (2003)361–365
29. Naik PK, Alam A, Malhotra A, & Rizvi O, Molecular Modeling and Structure-Activity Relationship of the Podophyllotoxin and Its Congeners. *J Biomol Screen,* **15** (2010) 528–540.
30. Santoshi S, Naik PK & Joshi HC, Rational design of novel anti-microtubule agent (9-azido-noscapine) from quantitative structure activity relationship (QSAR) evaluation of noscapinoids. *J Biomol Screen,* 9 (2011) 1047-1058.
31. Naik PK, Sindhura S T, & Singh H, Quantitative Structure-Activity Relationship (QSAR) of the Insecticides: The Development of Predictive In Vivo Insecticide Activity Models. *SAR QSAR Env Res,* **20** (2009) 551–556.